Inorganic Chemistry

ARTICLE

pubs.acs.org/IC

Study of the Conformationally Flexible, Wide Bite-Angle Diphosphine 4,6-Bis(3-diisopropylphosphinophenyl)dibenzofuran in Rhodium(I) and Palladium(II) Coordination Complexes

Keying Ding, Deanna L. Miller, Victor G. Young, Jr., and Connie C. Lu*

Department of Chemistry, University of Minnesota, 207 Pleasant Street SE, Minneapolis, Minnesota 55455-0431, United States

Supporting Information

ABSTRACT: The diphosphine 4,6-bis(3-diisopropylphosphinophenyl)dibenzofuran (abbreviated as ^{iPr}DPDBFphos) was prepared and studied for its potential as a *trans*-chelating ligand in transition-metal coordination complexes. In the rhodium norbornadiene complex [(^{iPr}DPDBFphos)Rh(NBD)]BF_4, which has been characterized with multinuclear NMR spectroscopy, X-ray crystallography, and electrochemical studies, the ligand binds in *cis* fashion. In the bis(acetonitrile) complexes of rhodium and palladium [(^{iPr}DPDBFphos)M(CH_3CN)$_2$](BF_4)$_n$ (M = Rh, Pd; n = 1, 2), the ligand adopts a *trans* coordination geometry. Density functional theory (DFT, M06-L) calculations predict that the *trans* conformer is energetically more favorable than the *cis* by 3.5 kcal/mol. Cyclic voltammograms of the bis(acetonitrile) Pd(II) and Rh(I) complexes contain reversible and quasi-reversible reduction events, respectively, which are preliminarily assigned as metal-based redox reactions.

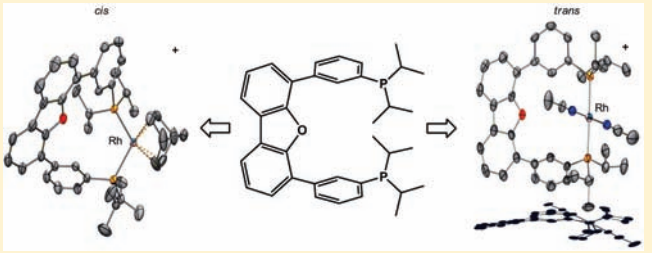

INTRODUCTION

Cis-chelating diphosphine ligands are featured prominently in homogeneous transition-metal catalysis, whereas *trans*-chelating diphosphines are uncommon. The latter are ill-suited to traditional d^8 square planar transition-metal catalysts because the two remaining sites at the metal center are opposed to one another, making it difficult to effect canonical catalytic steps such as migratory insertion and reductive elimination.[1,2] Instead, *trans*-chelating diphosphines may be interesting for penta- and hexacoordinate transition-metal catalysts by occupying the axial sites and leaving the equatorial sites open for substrate activation and conversion. In practice, however, "exclusively" *trans*-chelating diphosphines are challenging to design.[3] Even well-known *trans*-spanning diphosphines can support a large range of bite angles, including both *cis* and *trans* structures.[4] Nonetheless, these wide bite-angle diphosphines can be competent and even advantageous as an ancillary ligand for catalysis if the intermediate species can undergo *trans-cis* isomerization.[3,5−8] Current investigations seek to explore the unique role of *trans*-spanning diphosphines in homogeneous transition-metal catalysis.

Much past efforts have focused on the design and synthesis of *trans*-chelating diphosphines.[9] This task was initially challenging because of selectivity issues with metalating ligands wherein the two phosphine donors are separated by a sufficiently large distance. Competing reactions can form bimetallic and/or multimetallic products,[10] in which the diphosphine ligand bridges two transition-metal centers. The lack of binding selectivity can also manifest in product mixtures of both *cis* and *trans* mononuclear coordination complexes. Another potential problem is that sp^2 and sp^3 C−H bonds in the ligand backbone are susceptible to activation at the transition-metal center because of their proximity.[11] Typically, the more robust *trans*-spanning diphosphines contain relatively rigid backbones, such as the benzophenanthrene π-system in TRANSphos,[12] the fused spirobichroman rings in SPANphos,[13] or the biphenyl group in BISBI (Chart 1).[14] Another desirable design is to increase the distance between the ligand backbone and the phosphine donors so that any undesirable interactions between the transition metal center and the ligand backbone are minimized.[15] To achieve these criteria, we have prepared a unique, wide bite-angle diphosphine ligand featuring the diphenyldibenzofuran backbone, from which the general descriptor of these ligands as DPDBFphos is derived. We report here the synthesis of the diisopropyl-substituted phosphine derivative of DPDBFphos and its initial coordination chemistry with rhodium(I) and palladium(II).

RESULTS AND DISCUSSION

The two-step ligand synthesis from known starting materials is depicted in Scheme 1. The first step is a Suzuki coupling of the diboronic acid dibenzofuran-4,6-bis(boronic acid) and 2.2 equiv of 3-iodobromobenzene to give **1** in moderate yield (50%). Compound **1** is the ligand backbone with two reactive aryl bromide linkages. Next, the dibromide **1** is activated with 2 equiv of ^{n}BuLi via lithium-halogen exchange and subsequently quenched with diisopropylchlorophosphine to install the phosphine donors.

Received: November 29, 2010
Published: February 17, 2011

Chart 1. *trans*-Spanning Diphosphine Ligands with the Current Ligand Shown in Inset

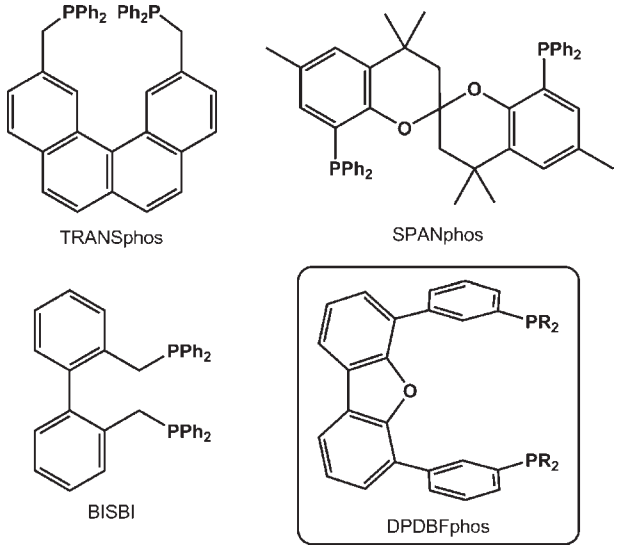

Scheme 1. Synthetic Route to the Diphosphine ^{iPr}DPDBFphos 2

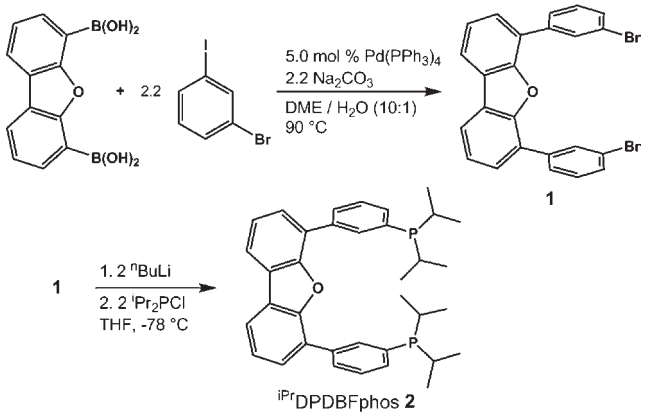

The diphosphine ligand **2**, which will be referred to as ^{iPr}DPDBFphos, was obtained in good yield (80%).

Initial metalation studies of the ligand focused on the noble transition metals because (1) we anticipated the metal−ligand complexes to be diamagnetic, which facilitates characterization by multinuclear NMR spectroscopy; (2) both rhodium and palladium diphosphine complexes are well-known catalysts for several bond-forming reactions; and (3) in specific cases, diphosphine ligands with wide bite angles (100 to 160°) have enhanced the efficiency of Pd-catalyzed C−C and C−N cross coupling reactions[5,6,8,15] or increased the regioselectivity in Rh-mediated hydroformylations.[16−18] Metalations of **2** with $[Rh(NBD)_2]BF_4$ (where NBD = norbornadiene) and $[Pd(MeCN)_4](BF_4)_2$ proceed cleanly to give $[(cis\text{-}^{iPr}DPDBFphos)Rh(NBD)]BF_4$ **3** and $[(trans\text{-}^{iPr}DPDBFphos)Pd(MeCN)_2](BF_4)_2$ **5**, respectively (Scheme 2). The coordination modes of the ligand in complexes **3**−**5** were determined by single-crystal X-ray diffraction studies (vide infra). Compound **3** is stable in acetonitrile at room temperature (rt); however, upon heating to 80 °C, the

Scheme 2. Synthetic Routes to ^{iPr}DPDBFphos Rh and Pd Complexes, 3 to 5

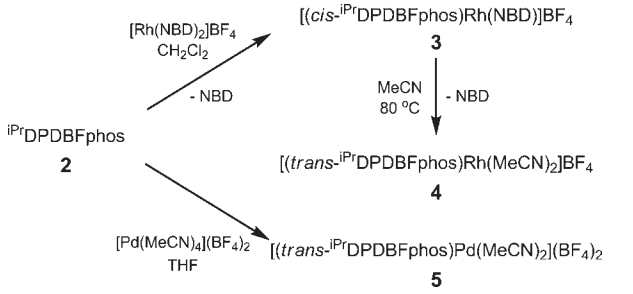

norbornadiene ligand exchanges readily with the solvent to form $[(trans\text{-}^{iPr}DPDBFphos)Rh(MeCN)_2]BF_4$ **4**. This reaction is unusual in that hydrogen is typically required to effect the overall exchange of norbornadiene with coordinating solvent molecules (or similarly weak donors) at (diphosphine)rhodium(I) centers. A notable exception is the direct substitution of NBD by an ether group at rhodium(I); however, in this case, the ether group was covalently linked to the phosphine ligand.[19]

The ^{31}P NMR spectra of **3**, **4**, and **5** are all consistent with chemically equivalent phosphorus nuclei. The ^{31}P chemical shifts are similar for the Rh and Pd bis(acetonitrile) complexes, **4** and **5**, respectively (^{31}P for **4** in $CDCl_3$: 46.4 ppm; **5** in CD_3CN: 43.1 ppm). The Rh norbornadiene complex **3** has an upfield phosphorus shift of 28.8 ppm, but this difference likely reflects the different binding modes of the ligand in the two Rh complexes (vide infra). The Rh−P coupling constants are also quite different for the two rhodium compounds, with J_{Rh-P} = 148 Hz for **3** and J_{Rh-P} = 127 Hz for **4**. The latter coupling constant falls into the expected range for Rh *trans*-diphosphine complexes (J_{Rh-P} = 118 to 135 Hz).[3] The Rh norbornadiene complex **3** exhibits a sharp proton NMR at room temperature (Supporting Information, Figure 1). In the ^{1}H NMR spectrum, half of the protons in the diphenyldibenzofuran backbone are unique. For the four isopropyl groups, only two distinct methyl resonances and one methine signal are observed; while for the norbornadiene ligand, three resonances are seen, one signal for each proton type. A C_{2v} symmetric structure is consistent with these NMR characteristics.

The room-temperature proton NMR spectra of the Rh and Pd bis(acetonitrile) compounds, **4** and **5**, respectively, are sharp in the aromatic region but broad in the aliphatic region. Upon cooling, these broad peaks sharpen, revealing two distinct methine protons and four methyls for the ligand isopropyl groups, as well as two additional methyl peaks, one for each bound acetonitrile. Except for these acetonitrile groups, exactly half of the protons in **4** are unique. Curiously, the two acetonitrile methyl shifts are dramatically different at 2.44 and 1.04 ppm in **4** ($CDCl_3$, −15 °C), signifying quite different chemical environments. Likewise, Figure 1 compares the ^{1}H NMR spectra of the palladium complex **5** in two solvents, CD_3CN and CD_2Cl_2, at room and low temperatures. Both room temperature spectra show extremely broad aliphatic peaks, which upon cooling to −30 °C in CD_3CN resolve nicely into two distinct methine and four unique methyl peaks. However, no signals for bound CH_3CN molecules are observed, likely because of the complete exchange of CD_3CN with the protio-solvent molecules at the palladium center. To obtain the chemical shifts of the bound

dx.doi.org/10.1021/ic102373w |*Inorg. Chem.* 2011, 50, 2545–2552

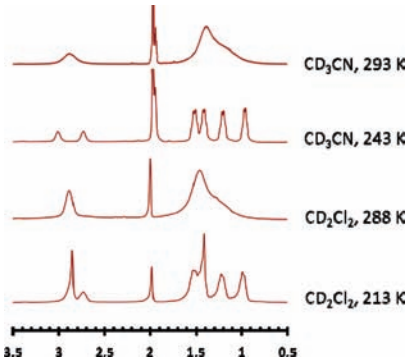

Figure 1. Variable-temperature proton NMR spectra (400 MHz) of [(^{iPr}DPDBFphos)Pd(NCMe)$_2$](BF$_4$)$_2$ **5** in CD_3CN and CD_2Cl_2.

acetonitrile molecules, the low temperature proton NMR experiment was performed in the non-coordinating solvent CD_2Cl_2. At −60 °C, the methyl peaks of the two bound CH_3CN molecules are observed at 2.84 and 1.40 ppm (along with some free CH_3CN at 1.97 ppm). Hence, in both the Pd and Rh bis(acetonitrile) compounds, a difference of ∼1.4 ppm is observed in the chemical shifts of the two acetonitrile methyl groups.

The fluxionality of the bis(acetonitrile) complexes **4** and **5** at room temperature suggests some torsional flexibility, that is, the N−M−N vector can rotate in the plane that is perpendicular to the P−M−P vector. Rotation can only partially occur since complete rotation of the N−M−N vector would result in collision between an acetonitrile molecule and the dibenzofuran backbone. Replacing acetonitrile with a bulkier nitrile analogue would further hinder this rotational freedom. To test this hypothesis, the corresponding ^{t}BuCN analogue of **4** was prepared by adding 2 equiv of ^{t}BuCN to **3**, and as anticipated, the resulting proton NMR spectrum (Supporting Information, Figure 2) is sharp at rt, with the four methyl and two methine signals all well-resolved. Interestingly, the ^{t}Bu protons are shifted by over 1 ppm (1.41, 0.34 ppm, $CDCl_3$, 300 MHz). For comparison, the ^{t}Bu protons in free ^{t}BuCN are observed at 1.35 ppm.

Molecular Structures from X-ray Crystallography. Compound **3** can be crystallized from various solvent combinations, but single crystals of sufficient quality for X-ray diffraction studies were obtained from vapor diffusion of benzene into a 1,2-difluorobenzene solution (Figure 2). Single crystals of **4** and **5** were grown from their concentrated acetonitrile solutions by cooling to −25 °C or vapor diffusion of ether at rt, respectively. Crystallographic details are given in Table 1. In the trio of crystal structures, all metal centers have square planar geometry with the ^{iPr}DPDBFphos ligand occupying either *cis*- or *trans*-binding sites.

In the bis(acetonitrile) complexes, the ligand is a *trans* chelator with P−M−P angles of 177.39(4)° in **4** (Figure 3) and 174.59(3)° in **5** (Figure 4). Molecular structures of bis(acetonitrile) Rh and Pd complexes are uncommon with two phosphine donors and rare for the more restrictive case of *trans*-chelating phosphines. The only exception is Chisholm's [*trans*-(PCy$_3$)$_2$Rh(MeCN)$_2$]BF$_4$ complex,[20] and its Rh−P and Rh−N bond distances of 2.341(2) and 1.984(2) Å, respectively, compare reasonably with those of **4** (ave. Rh−P 2.304 Å, ave. Rh−N 1.966 Å). An approximate mirror plane that bisects the P−P vector and contains the oxygen atom of the dibenzofuran backbone equalizes the two halves of the molecule. The bound acetonitriles, which lie in the mirror plane, are inequivalent with

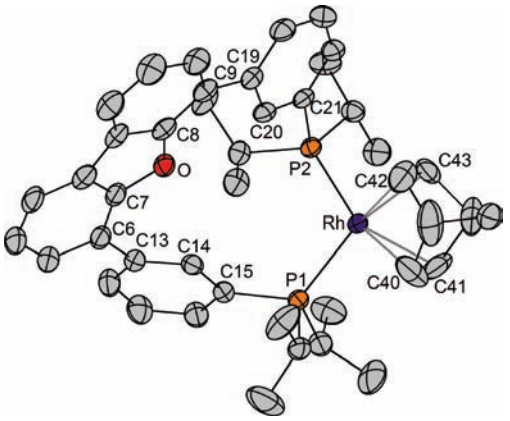

Figure 2. Solid-state structure of the cation [(^{iPr}DPDBFphos)Rh(NBD)] **3** at 50% probability level. Hydrogen atoms, BF$_4$ counteranion, and extra solvent molecules were omitted for clarity. Selected bond distances (Å): Rh−P1 2.3887(9), Rh−P2 2.3524(9), Rh−C40 2.204(5), Rh−C41 2.190(5), Rh−C42 2.160(4), Rh−C43 2.159(4); selected bond angle (deg): P1−Rh−P2 104.52(3); selected torsion angles (deg): Rh−P1−C15−C14 −54.3(3), Rh−P2−C21−C20 −73.3(2), C7−C6−C13−C14 34.3(5), C8−C9−C19−C20 −14.6(5).

N2 situated near the dibenzofuran backbone while N1 is spatially directed toward the isopropyl groups.

Space-filling images of structures **4** and **5** reveal that the CH_3C group attached to N2 is sandwiched between the π-systems of the two aryl linkers, which are slightly canted relative to the dibenzofuran backbone (Supporting Information, Figure 3). In these two structures, the distance between the carbon atom of the methyl group and the centroids of the aryl linker rings ranges from 3.857 to 4.283 Å. This is indeed significant since the total sum of a methyl C−H bond (1.0 Å), the van der Waal radius of a π-system (1.7 Å), and that of a hydrogen atom (1.2 Å) is roughly 3.9 Å. The ring current associated with these aryl linkers should shield this methyl group,[21] which explains the upfield shift of one of the acetonitrile methyl resonances by ∼1.4 ppm in the proton NMR spectra of **4** and **5**. The coalescence of the isopropyl resonances in the proton NMR spectrum at room temperature reflects slow exchange of the two acetonitrile molecules as well as the ligand isopropyl groups. The fluxional process is likely a combination of some torsional rotation of the N−M−N vector and back-and-forth canting of the aryl linkers as shown in Scheme 3. In the ^{t}BuCN analogue of **4**, the aryl linkers, would be effectively locked in place because of unfavorable steric interactions with the bulkier ^{t}Bu group.

The crystal structure of the Rh norbornadiene complex **3** stands apart in that the diphosphine ligand is a *cis* chelator with a P−Rh−P angle of 104.52(3)°. The Rh center is slightly distorted from square planar geometry with a small twist angle between the two Rh-ligand planes (P−Rh−P and Rh(NBD)) of 12.8°. While crystal structures of (diphosphine)Rh(NBD) cations are common, it is rare to find such structures featuring wide bite-angle diphosphines. Indeed, among the 66 known examples in the Cambridge Structural Database,[22] the average P−Rh−P bond angle is 89.8° with a standard deviation of 5.8°. The bite angles range from 82.9 to 103.7°. Hence, even as the *cis* conformer, ^{iPr}DPDBFphos would be well considered a wide bite-angle diphosphine. The Rh−P and Rh−C bond distances are not remarkable among this set. The former (2.3887(9), 2.3524(9) Å) are slightly longer than the average (2.31 Å, SD = 0.04), and the

dx.doi.org/10.1021/ic102373w |*Inorg. Chem.* 2011, 50, 2545–2552

Table 1. Crystallographic Data for 3−5

	3·0.64(C_6H_6) ·0.36($C_6H_4F_2$)	4·2(CH_3CN)	5·CH_3CN
formula	$C_{49}H_{55.3}BF_{4.7}OP_2Rh$	$C_{44}H_{54}BF_4N_4OP_2Rh$	$C_{42}H_{51}B_2F_8N_3OP_2Pd$
crystal size, mm^3	0.45 × 0.30 × 0.20	0.40 × 0.30 × 0.20	0.40 × 0.30 × 0.20
fw, g/mol	925.19	904.93	955.82
space group	$P\bar{1}$	*Pbca*	$P2_1/n$
a, Å	12.888(1)	25.253(6)	11.5799(9)
b, Å	13.145(1)	11.484(3)	11.3663(9)
c, Å	14.702(2)	30.963(7)	33.729(3)
α, deg	103.481(2)	90	90
β, deg	108.628(2)	90	95.942(2)
γ, deg	104.214(2)	90	90
V, $Å^3$	2153.0(4)	8979(3)	4415.5(6)
Z	2	8	4
T, K	173(2)	0.71073(2)	0.71073(2)
ρ calcd. g cm^{-3}	1.427	1.339	1.438
refl. collected/$2\sigma_{max}$	81982/55.0	82062/50.1	42213/50.1
unique refl./$I > 2\theta(I)$	9711/6233	7955/6217	7836/6233
no. params./restraints	584/168	522/6	556/6
λ, Å /*μ* (Kα), mm^{-1}	0.71073/0.528	0.71073/0.505	0.71073/0.563
R1/GooF	0.0458/1.048	0.0537/1.296	0.0419/1.045
wR2 ($I > 2\sigma(I)$)	0.0984	0.1669	0.0890
residual density, e $Å^{-3}$	0.725/−0.631	1.347/−0.695	1.108 /−0.556

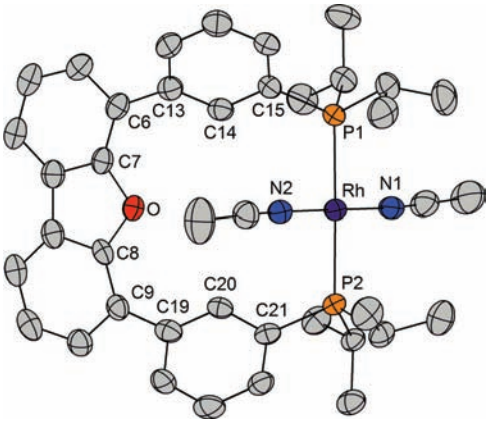

Figure 3. Solid-state structure of the cation [(^{iPr}DPDBFphos)Rh(NCMe)$_2$] **4** at 50% probability level. Hydrogen atoms, BF_4 counteranion, and extra solvent molecules were omitted for clarity. Selected bond distances (Å): Rh−P1 2.309(1), Rh−P2 2.299(1), Rh−N1 1.964(4), Rh−N2 1.968(4); selected bond angles (deg): P1−Rh−P2 177.39(4), N1−Rh−N2 179.1(2), P1−Rh−N1 90.0(1), P1−Rh−N2 90.0(1), P2−Rh−N1 92.5(1), P2−Rh−N2 87.4(1); selected torsion angles (deg): Rh−P1−C15−C14 −45.4(4), Rh−P2−C21−C20 35.3(4), C7−C6−C13−C14 43.8(7), C8−C9−C19−C20 −43.1(6).

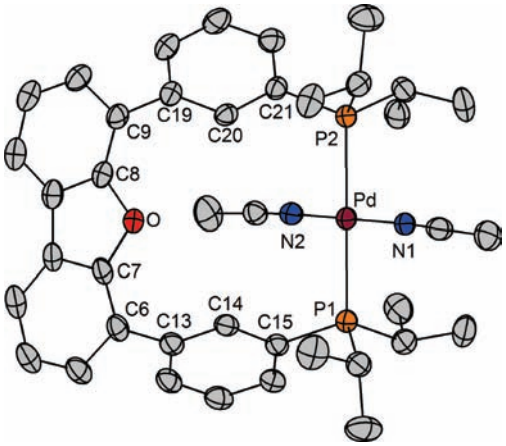

Figure 4. Solid-state structure of the dication [(^{iPr}DPDBFphos)Pd(NCMe)$_2$] **5** at 50% probability level. Hydrogen atoms, BF_4 counteranions, and extra solvent molecules were omitted for clarity. Selected bond distances (Å): Pd−P1 2.3594(9), Pd−P2 2.3521(9), Pd−N1 2.002(3), Pd−N2 1.963(3); selected bond angles (deg): P1−Pd−P2 174.59(3), N1−Pd−N2 178.0(1), P1−Pd−N1 91.68(8), P1−Pd−N2 87.65(8), P2−Pd−N1 92.41(8), P2−Pd−N2 88.14(8); selected torsion angles (deg): Pd−P1−C15−C14 −49.5(3), Pd−P2−C21−C20 45.1(3), C7−C6−C13−C14 52.1(5), C8−C9−C19−C20 −50.5(5).

latter (2.204(5), 2.190(5), 2.160(4), 2.159(4) Å) are slightly shorter (2.21 Å, SD = 0.03), but they are all within one or two standard deviation(s) of their corresponding average values.

The structure of **3** has no clear symmetry elements, although within the molecular fragment "(^{iPr}DPDBFphos)Rh" (i.e., ignoring NBD), a 2-fold rotation axis is present that contains the Rh and O atoms. The ligand backbone is twisted so that the torsion angle defined by (aryl)C−P−P−C(aryl) is 87.0°. In contrast, this torsion angle is only 9.3° in the *trans* compound **4**. The observation of just two distinct methyl resonances for the isopropyl groups in **3** (versus four in **4**) by NMR belies the asymmetry of the solid-state structure. Rotation along both Rh−P bonds with concurrent adjustment of the phosphine substituents would effectively swing the P_2Rh(NBD) fragment back and forth relative to the dibenzofuran frame. If such a motion is rapid, then the averaged molecule would appear to have C_{2v} symmetry, which is consistent with its proton NMR spectrum.

Cyclic Voltammetry. The electrochemical behavior of complexes **3**, **4**, and **5** was investigated with cyclic voltammetry.

dx.doi.org/10.1021/ic102373w |*Inorg. Chem.* 2011, 50, 2545–2552

Scheme 3. Fluxional Processes That Exchange the Two Bound Acetonitrile Molecules, Represented Simply as L_1 and L_2, in [(*trans*-^{iPr}DPDBFphos)Rh(NCMe)$_2$]BF$_4$ 4

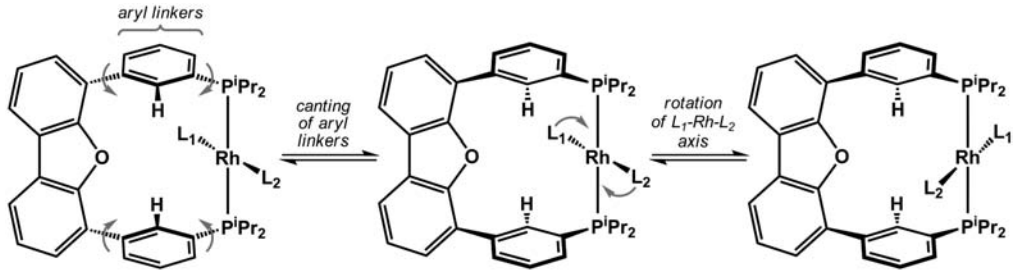

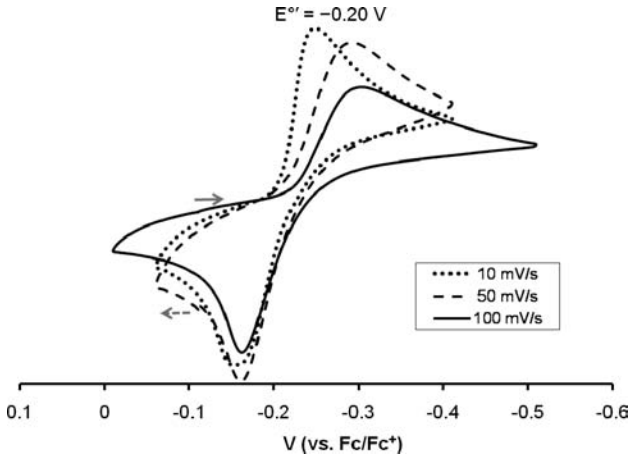

Figure 5. Cyclic voltammograms of [(^{iPr}DPDBFphos)Pd(NCMe)$_2$](BF$_4$)$_2$ **5** at various scan rates (10, 50, 100 mV/s; 0.1 M [^{n}Bu$_4$N]PF$_6$ in MeCN). Currents were multiplied by (scan rate)$^{-1/2}$.

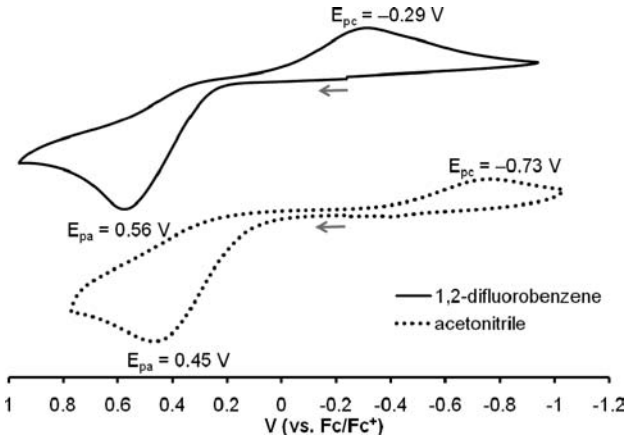

Figure 6. Stacked cyclic voltammograms of [(^{iPr}DPDBFphos)Rh(NCMe)$_2$](BF$_4$)$_2$ **4** in 1,2-difluorobenzene and acetonitrile (100 mV/s; 0.1 M [^{n}Bu$_4$N]PF$_6$).

Figure 5 shows the CV of the Pd complex **5** in 0.1 M [^{n}Bu$_4$N]PF$_6$ acetonitrile solution at various scan rates (10, 50, 100 mV/s). Scanning at 10 mV/s, a quasi-reversible electron-transfer wave is observed at −0.20 V with a peak-to-peak separation of 90 mV (vs Fc/Fc$^+$). At the faster scan rate of 100 mV/s, the peak potential shifts cathodically to −0.23 V while the peak-to-peak separation increases to 135 mV. This trend is consistent with a quasi-reversible process wherein the electron-transfer kinetics are sufficiently slow so that at faster scan rates the redox event appears less reversible. Because Pd(II) is well-known to undergo reduction to Pd(0) during catalysis, this event is assigned as a Pd(II)/Pd(0) redox couple.

Figure 6 shows the cyclic voltammogram of the Rh bis(acetonitrile) complex **4** in two different solvents, acetonitrile and 1,2-difluorobenzene. Sullivan and Meyer have previously demonstrated the utility of 1,2-difluorobenzene as an inert and non-coordinating solvent in electrochemical studies of transition metal complexes that bind solvent molecules as ligands during electrochemical experiments.[23] In both solvents, an irreversible oxidative event is observed near 500 mV. This oxidative event is followed by an irreversible reductive feature that shifts dramatically in the different solvents, −0.29 V in 1,2-difluorobenzene and −0.73 V in acetonitrile. We speculate that the irreversible feature near 0.5 mV is a two-electron oxidation of Rh(I) to Rh(III), a common oxidation state for mononuclear Rh complexes. However, oxidation to a mononuclear Rh(II) species is also possible.[24,25]

Recording cyclic voltammograms of the Rh norbornadiene complex **3** in acetonitrile proved unsuccessful because after only a few cycles, the voltammograms were remarkably similar to that of **4**, the Rh bis(acetonitrile) complex. Henceforth, the cyclic voltammograms were collected in 1,2-difluorobenzene with 0.1 M [^{n}Bu$_4$N]PF$_6$. Surprisingly, in contrast to **4**, no oxidative events were observed, and instead, a reduction was seen at −1.66 V versus Fc/Fc$^+$ (Figure 7). A full sweep of the ligand ^{iPr}DPDBFphos was recorded as a control (Supporting Information, Figure 4), and none of these events is ascribable to the ligand. Hence, this feature is tentatively assigned as a Rh(I)/Rh(0) redox couple. The reduction is best described as quasi-reversible because the current ratio i_{pc}/i_{pa} approaches unity only at sufficiently fast scan rates (>500 mV/s) while the i_{pa} of the corresponding secondary oxidation at −0.5 V diminishes. This scan-rate behavior may be consistent with an unstable product that is generated electrochemically, which then converts into another species at a rate comparable to that of the experimental time scale.

Theoretical Calculations. Because metalation reactions of ^{iPr}DPDBFphos produced both *cis* and *trans* coordination complexes, we were interested in unraveling the ligand's inherent propensity to adopt one conformation over the other via theoretical investigations. Casey and Whiteker previously studied the natural bite angle of chelating diphosphines using molecular mechanics calculations.[26] The work has been continued by van Leeuwen,[4] but more recently he has reported that MM2 calculations can give gross errors in determining bite angles.[27]

dx.doi.org/10.1021/ic102373w |*Inorg. Chem.* 2011, 50, 2545–2552

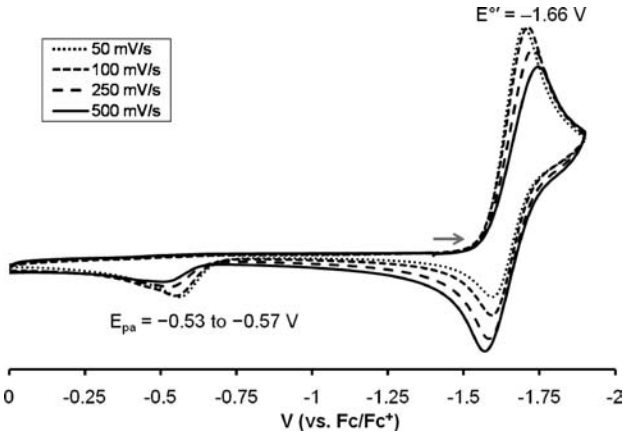

Figure 7. Cyclic voltammograms of $[(^{iPr}DPDBFphos)Rh(NBD)]BF_4$ **3** at various scan rates (50, 100, 250, 500 mV/s; 0.1 M $[^nBu_4N]PF_6$ in 1,2-difluorobenzene). Currents were multiplied by (scan rate)$^{-1/2}$.

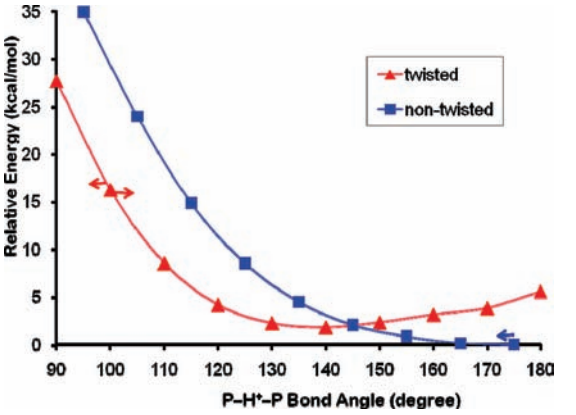

Figure 8. Relaxed potential energy scan of various bite angles for ^{iPr}DPDBFphos in the model cation $[(^{iPr}DPDBFphos)H]^+$. Two landscapes, twisted and non-twisted, were calculated independently from the initial geometries of the *cis* and *trans* structures, respectively (indicated by arrows).

For the specific case of SPANphos, van Leeuwen applied semiempirical (AM1) and DFT (B3LYP) methods, but the ligand conformational space was explored only for the spirobichroman backbone, and the phosphine groups were omitted entirely.[27] These studies were complemented with calculations of the ligand−metal complex, but the latter cannot disentangle the ligand's inherent preference from the electronic/geometric bias of the metal center.

We chose to model the protonated ligand $[H(^{iPr}DPDBFphos)]^+$ to minimize the electronic bias of the connecting atom by using a spherical partner. Akin to Casey's calculations, the P−H bond distances were kept constant at 2.30 Å to mimic the Rh−P bond distance. The initial geometries were taken from the solid-state structures of $[(cis\text{-}^{iPr}DPDBFphos)Rh(NBD)]BF_4$ **3** and $[(trans\text{-}^{iPr}DPDBFphos)Rh(MeCN)_2](BF_4)_2$ **4**. A relaxed potential energy scan was performed with geometry optimizations at each step for a targeted range of bite angles, ∼90 to 180 degrees with a step size of 10 degrees. We employed the M06-L DFT functional in the Gaussian09 program because it has been reported to give more accurate energies for non-covalent interactions and transition metal systems compared to B3LYP.[28]

The plot of relative total energy versus bite angle is shown in Figure 8. Two landscapes were computed. The twisted landscape was computed using the *cis* structure **3**, and the non-twisted landscape was computed with the *trans* analogue **4**. For the former, a shallow potential well is calculated with a minimum at 140 degrees. The minimum of the non-twisted landscape occurs at 180 degrees and is 1.78 kcal/mol lower in energy than the twisted minimum. In both landscapes, the accessible bite angle range (within 3 kcal/mol) is large, from 140 to 180 degrees for the non-twisted geometry and 120 to 170 degrees for the twisted geometry. However, it is likely that the energies for the twisted landscape are overestimated (vide infra).

Single point energy calculations were also performed to compare the ligand conformations in the two structures of **3** and **4**. First, the geometry of the two complexes were optimized (M06-L, def2-TZVP for Rh, P, N, def2-SV(P) for C, H, O). In both compounds, the calculated Rh−P bond distances were comparable to experimental values (within 0.04 Å), the Rh−C/Rh−N bond distances within 0.01 Å, and the P−Rh−P bond angles within 4 degrees. Next, all atoms except those comprising ^{iPr}DPDBFphos were deleted, and single point energies were calculated. The *trans* conformer was lower in energy than the *cis* by 3.5 kcal/mol.

Future Outlook. A conformationally flexible diphosphine ligand is reported that can bind to a transition metal center in both *trans* and *cis* modes. DFT calculations indicate that a changeover from *cis* to *trans* geometry can provide a 3.5 kcal/mol driving force. This may be the underlying reason why the conversion of $[(cis\text{-}^{iPr}DPDBFphos)Rh(NBD)]^+$ compound to the corresponding *trans* bis(acetonitrile) complex does not require hydrogen to remove the norbornadiene group, and instead occurs by ligand exchange. Future directions will seek to couple the driving force associated with *cis*-to-*trans* conversion to metal-mediated reactivity. Cyclic voltammograms suggest the feasibility of zero-valent Rh and Pd species, and ongoing work is focused on preparing reduced coordination complexes.

EXPERIMENTAL SECTION

General Considerations. Unless otherwise stated, all manipulations were performed under a dinitrogen atmosphere in a VAC Atmosphere glovebox or using standard Schlenk techniques. Standard solvents were deoxygenated by sparging with dinitrogen and dried by passing through activated alumina columns of a SG Water solvent purification system. 1,2-Difluorobenzene was degassed, dried with activated alumina (8−14 mesh size), and stored over activated 4 Å molecular sieves. Deuterated solvents were purchased from Cambridge Isotope Laboratories, Inc., degassed via freeze−pump−thaw cycles, and stored over activated 4 Å molecular sieves. Proton, ^{13}C, and ^{31}P NMR spectra were recorded on Varian 300, 400, and 500 MHz spectrometers at ambient temperature unless otherwise stated. Chemical shifts were referenced to residual solvent, except for ^{31}P NMR data, for which an external reference of 85% H_3PO_4 set to 0 ppm was used. Because of the proton equivalence within these systems, the reported integrations should be doubled to match the expected absolute values. Elemental analyses were performed by Columbia Analytical Services. The ligand precursor dibenzofuran-4,6-bis(boronic acid)[29] and the metal precursor $[Pd(CH_3CN)_4](BF_4)_2$[30] were prepared according to published procedures.

*4,6-Bis(3-bromophenyl)dibenzofuran (**1**).* Dibenzofuran-4,6-bis(boronic acid) (4.59 g, 17.94 mmol), 3-iodobromobenzene (11.16 g, 39.46 mmol), $Pd(PPh_3)_4$ (1.04 g, 0.90 mmol), Na_2CO_3 (4.25 g, 40 mmol), DME (280 mL), and deoxygenated dH_2O (28 mL) were combined in a 500 mL resealable flask. The flask was sealed, and the

dx.doi.org/10.1021/ic102373w |*Inorg. Chem.* 2011, 50, 2545–2552

mixture was heated at 90 °C for 12 h. After the reaction solution cooled to rt, the solvent was removed under reduced pressure, and the remaining residue was dissolved in benzene (250 mL), stirred for 30 min, and washed with water (3 × 50 mL) in a separatory flask under air. The organic layer was separated, dried over $MgSO_4$, and filtered through an alumina plug to produce a colorless solution. The solvent was removed under reduced pressure to give a white powder (4.46 g, 50% yield). ^{1}H NMR (300 MHz, $CDCl_3$): δ 8.12 (br t, J = 1.5 Hz, 1H), 7.98 (dd, J = 7.5 and 0.9 Hz, 1H), 7.93 (ddd, J = 7.8, 0.9, and 0.6 Hz, 1H), 7.65 (dd, J = 7.5 and 0.9 Hz, 1H), 7.55 (dq, J = 8.1 and 0.9 Hz, 1H), 7.45 (app q, J = 7.8 Hz, 2 H). ^{13}C NMR (75.5 MHz, $CDCl_3$): δ 153.3, 138.3, 131.7, 130.9, 130.5, 127.4, 126.8, 125.1, 124.3, 123.8, 123.0, 120.7.

*4,6-Bis(3-diisopropylphosphinophenyl)dibenzofuran (^{iPr}DPDBFphos, **2**).* To a solution of **1** (1.59 g, 3.32 mmol) in THF (100 mL) cooled in a dry ice/acetone bath, ^{n}BuLi (4.15 mL, 6.64 mmol, 1.6 M in hexane) was added dropwise. The bright yellow mixture was stirred at −78 °C for 1.5 h and then quenched slowly with diisopropylchlorophosphine (1.06 mL, 6.64 mmol). The resulting colorless solution was stirred for 4 h at −78 °C and then evaporated to dryness under reduced pressure. After moving into a glovebox, the residue was extracted with diethyl ether (100 mL) and filtered through a plug of Celite. Colorless crystals (1.45 g, 80% yield) were obtained by cooling an Et_2O/pentane solution (15 mL, 2:1) to −25 °C. ^{31}P NMR(121 MHz, $CDCl_3$): δ 12.3. ^{1}H NMR (500 MHz, $CDCl_3$): δ 8.01 (m, 1H), 8.00 (dd, J = 7.5 and 1.0, 1H), 7.93 (d, J = 7.5 Hz, 1H), 7.65 (dd, J = 7.5 and 1.0 Hz, 1H), 7.53 (m, 2H), 7.48 (app t, J = 8 Hz, 1H), 2.15 (septet of d, PC*H*$(CH_3)_2$, $^3J_{HH}$ = 7.0, $^2J_{HP}$ = 2.0 Hz, 2H), 1.13 (dd, PCH(CH_3C′H_3), $^3J_{HP}$ = 15 Hz, $^3J_{HH}$ = 7.0 Hz, 6H), 0.97 (dd, PCH(CH_3C′H_3), $^3J_{HP}$ = 11.0 Hz, $^3J_{HH}$ = 7.0 Hz, 6H). ^{13}C NMR (126 MHz, $CDCl_3$): δ 153.5, 136.1 (d, J = 8 Hz), 135.4 (d, J = 18 Hz), 134.7 (d, J = 20 Hz), 133.8 (d, J = 17 Hz), 129.6, 128.3 (d, J = 7 Hz), 127.4, 126.0, 125.2, 123.5, 119.9, 23.0 (d, J = 11 Hz), 20.1 (d, J = 18 Hz), 19.1 (d, J = 9 Hz). ESI-HRMS-TOF m/z: $[M + H]^+$ calc. for $C_{36}H_{43}OP_2$, 553.2789; found, 553.2813.

*[(^{iPr}DPDBFphos)Rh(NBD)]BF_4 (**3**).* A 20 mL scintillation vial was charged with **2** (101 mg, 183 μmol), $Rh(NBD)_2(BF_4)$ (68 mg, 183 μmol) and 15 mL CH_2Cl_2. The red solution was stirred at rt for 4 h and then evaporated to dryness under reduced pressure. The residue was washed with diethyl ether (2 × 5 mL) to give a red-orange powder (134 mg, 90% yield). Crystals were grown from vapor diffusion of pentane into a $CHCl_3$ solution of **3**. Single crystals suitable for X-ray analysis were obtained from vapor diffusion of C_6H_6 into a 1,2-difluorobenzene solution of **3** at rt. ^{31}P NMR(121 MHz, $CDCl_3$): δ 28.8 (d, J_{RhP} = 148 Hz). ^{1}H NMR (500 MHz, $CDCl_3$): δ 8.44 (br d, J = 8.5 Hz, 1H), 8.06 (dd, J = 8.0 and 1.0 Hz, 1H), 7.82 (d, J = 7.5 Hz, 1H), 7.77 (d, J = 7.5 Hz, 1H), 7.70 (t, J = 7.5 Hz, 1H), 7.66 (br t, J = 7.0 Hz, 1H), 7.54 (t, J = 7.8 Hz, 1H), 5.08 (br, 2H, *NBD*), 4.05 (br, 1H, *NBD*), 2.35 (br, 2H, PC*H*CH_3CH_3′), 1.89 (s, 1H, *NBD*), 1.29 (br, 6H, PCH(CH_3C′H_3), 1.02 (br, 6H, PCH (CH_3C′H_3). ^{13}C NMR (75.5 MHz, CD_2Cl_2): δ 153.5, 136.9 (t, J = 5.0 Hz), 133.4 (t, J = 6.3 Hz), 131.8 (m), 130.9, 130.1, 130.0, 126.7, 125.3, 124.5, 124.4, 121.4, 75.6, 69.0, 53.5, 26.5 (m, J = 9.8 Hz), 21.4, 20.4. ESI-MS(+): m/z = 747 $[(M - BF_4)^+]$. Anal. Calcd. for $C_{43}H_{50}BF_4OP_2Rh$: C, 61.89; H, 6.04; N, 0. Found: C, 62.09; H, 5.92; N, 0.0.

*[(^{iPr}DPDBFphos)Rh(CH_3CN)$_2$]BF_4 (**4**).* Compound **3** (110 mg, 132 μmol) was dissolved in acetonitrile (10 mL) and heated for 2 h at 80 °C. All volatiles were evaporated under reduced pressure. The residue was washed with diethyl ether (3 × 3 mL) and dried under reduced pressure, affording a bright yellow powder (93 mg, 85% yield). Yellow needle crystals were grown from concentrated acetonitrile solution at −25 °C. ^{31}P NMR(121 MHz, $CDCl_3$): δ 46.4 (d, J_{RhP} = 127 Hz). ^{1}H NMR (500 MHz, $CDCl_3$): δ 8.57 (br t, J = 5.0 Hz, 1H), 8.08 (dd, J = 6.0 and 3.0 Hz, 1H), 7.63 (d, J = 8.0 Hz, 1H), 7.58 (t, J = 8.0 Hz, 1H), 7.53 (m, 2H), 7.45 (m, 1H), 2.53 to 2.35 (br m's, 3.5H, methine of P^{i}Pr$_2$ and Rh(CH_3-CN)(C′H_3CN)), 1.45 to 0.95 (br m's, 13.5H, methyl of P^{i}Pr$_2$ and Rh(CH_3CN)(C′H_3CN)). The broad peaks in the aliphatic region sharpened upon cooling to −15 °C. However, the aryl peaks grew broader with decreasing temperature, so their chemical shifts will not be reported with the low temperature characterization. ^{1}H NMR(400 MHz, $CDCl_3$, −15 °C): δ 2.62 (br, 1H, methine of P^{i}Pr$_2$), 2.44 (s, 1.5H, Rh(*CH*$_3$CN)(C′H_3CN)), 2.26 (br m, 1H, methine of P^{i}Pr$_2$), 1.43 (br, 3H, methyl of P^{i}Pr$_2$), 1.33 (br, 3H, methyl of P^{i}Pr$_2$), 1.17 (br, 3H, methyl of P^{i}Pr$_2$), 1.04 (s, 1.5H, Rh(CH_3CN)(C′H_3CN)), 0.92 (br, 3H, methyl of P^{i}Pr$_2$). ^{13}C NMR (101 MHz, CD_2Cl_2): δ 153.6, 138.3 (t, J = 10.2 Hz), 137.4 (t, J = 6.6 Hz), 131.5, 131.2, 130.8, 129.4, 127.9 (t, J = 16 Hz), 126.2, 125.9, 124.4, 120.6, 23.0 to 22.0 (br m), 20.4 (br m), 18.9 (br), 15.6 (br), 4.3 to 3.0 (br m). At rt, the aliphatic carbon peaks were not well-resolved. ESI-MS(+): m/z = 737 $[(M - BF_4)^+]$. Anal. Calcd. for $C_{40}H_{48}BF_4N_2OP_2Rh$: C, 58.27; H, 5.87; N, 3.40. Two independent crystalline samples were tested. Found: (first) C, 58.81; H, 6.00; N, 4.05; (second) C, 58.88; H, 6.34; N, 3.72.

*[(^{iPr}DPDBFphos)Pd(CH_3CN)$_2$](BF_4)$_2$ (**5**).* The ligand **2** (58 mg, 106 μmol) and $[Pd(CH_3CN)_4](BF_4)_2$ (47 mg, 106 μmol) were dissolved in tetrahydrofuran (THF) and stirred overnight at rt. All volatiles were removed under reduced pressure. The residue was rinsed with diethyl ether and dried under reduced pressure, affording a pale yellow solid (157 mg, 80% yield). Pale yellow needle crystals were grown from vapor diffusion of Et_2O into a CH_3CN solution of **5**. ^{31}P NMR (202 MHz, CD_3CN): δ 43.1. ^{1}H NMR (500 MHz, CD_3CN): δ 8.55 (br t, J = 5 Hz, 1H), 8.25 (dd, J = 3.6 and 5.7 Hz, 1H), 7.92 (d, J = 7.8 Hz, 1H), 7.79 (t, J = 7.8 Hz, 1H), 7.712 (m, 1H), 7.61 (m, 2H), 3.08 to 2.69 (br m's, 3.5 H, P(C*H*$(CH_3)_2)_2$ and Pd(C*H*$_3$CN)(C′H_3CN)), 1.72 to 0.80 (br m's, 13.5H, P($CH(CH_3)_2)_2$ and Pd(CH_3CN)(C′H_3CN). The broad peaks in the aliphatic region sharpen upon cooling down to −60 °C. Only the aliphatic resonances are reported at the lower temperature as the aryl peaks do not shift significantly. ^{1}H NMR (400 MHz, CD_2Cl_2, −60 °C): δ 2.86 (br, 1H, methine of P^{i}Pr$_2$), 2.86 (s, 1.5 H, Pd(*CH*$_3$CN)-(C′H_3CN)), 2.74 (br, 1H, methine of P^{i}Pr$_2$), 1.53(br, 3H, methyl of P^{i}Pr$_2$), 1.42 (s, 1.5 H, Pd(CH_3CN)(C′H_3CN)), 1.23 (br, 3H, methyl of P^{i}Pr$_2$), 1.00 (br, 3H, methyl of P^{i}Pr$_2$).^{13}C NMR (75 MHz, CD_3CN): δ 154.0, 139.1 (t, J = 6.3 Hz), 137.1 (t, J = 8.6 Hz), 134.3, 132.8, 131.5, 131.3 (t, J = 4.0 Hz), 126.3, 125.9, 125.3, 122.6, 122.3, 122.1, 24.1 (t, J = 12.6 Hz), 21.7 to 19.2 (br, m), 18.7, 18.3 to 15.1 (br, m). At rt, the aliphatic carbon peaks were not well-resolved. ESI-MS (+): m/z = 740 $[(M - BF_4)^+]$. Anal. Calcd. for $C_{42}H_{51}B_2F_8N_3OP_2Pd$ (**5** + CH_3CN): C, 52.77; H, 5.38; N, 4.40. Found: C, 52.68; H, 5.17; N, 4.33.

X-ray Crystallographic Data Collection and Refinement of the Structures. Single crystals of **3** to **5** were placed onto the tip of a 0.1 mm diameter glass capillary and mounted on a Bruker SMART Platform CCD diffractometer for data collection at 173(2) K. The data collection was carried out using MoKα radiation (graphite monochromator). The data intensity was corrected for absorption and decay (SADABS).[31] Final cell constants were obtained from least-squares fits of all measured reflections. The structure was solved using SHELXS-97 and refined using SHELXL-97.[32] A direct-methods solution was calculated which provided most non-hydrogen atoms from the E-map. Full-matrix least-squares/difference Fourier cycles were performed to locate the remaining non-hydrogen atoms. All non-hydrogen atoms were refined with anisotropic displacement parameters. Hydrogen atoms were placed in ideal positions and refined as riding atoms with relative isotropic displacement parameters. Crystallographic data for compounds **3** to **5** are listed in Table 1.

Physical Methods. Mass spectrometry (MS) data was acquired on a Bruker BioTOF ESI-MS under positive mode. Cyclic voltammetry experiments were performed inside a glovebox with a CHInstruments Model 600D potentiostat/galvanostat. A single-chamber cell was set up with a glassy carbon working electrode (3 mm diameter), a Pt wire as the auxiliary electrode, and a reference electrode consisting of a silver wire in 10 mM $AgNO_3$ solution (0.1 M $[^nBu_4N]PF_6$ in CH_3CN). All measurements were calibrated to an internal ferrocene standard.

dx.doi.org/10.1021/ic102373w |*Inorg. Chem.* 2011, 50, 2545–2552

Theoretical Calculations. Geometry optimizations and single-point energy calculations were performed using the Gaussian09 program[33] and the M06-L functional.[34] The all-electron Gaussian basis sets used were those reported by the Ahlrichs group. For rhodium, nitrogen, and phosphorus atoms, triple-ζ-quality basis sets with one set of polarization functions were used (def2-TZVP) with additional ECP bases for rhodium.[35] The carbon, oxygen, and hydrogen atoms were described by smaller polarized split-valence def2-SV(P) basis sets.[36]

■ ASSOCIATED CONTENT

Supporting Information. Additional spectroscopic and theoretical data, including the proton NMR spectra of $[(^{iPr}DPDBFphos)Rh(NBD)]BF_4$ **3** and $[(^{iPr}DPDBFphos)Rh(NC^tBu)_2]BF_4$, crystallographic details of complexes **3**−**5**, and cyclic voltammogram of $^{iPr}DPDBFphos$. This material is available free of charge via the Internet at http://pubs.acs.org.

■ AUTHOR INFORMATION

Corresponding Author
*E-mail: clu@umn.edu.

■ ACKNOWLEDGMENT

The authors gratefully acknowledge Dr. Benjamin Lynch, Dr. Nicholas Labello, Dr. Boris Averkiev, and the Minnesota Supercomputing Institute for computing support/resources. Elodie Marlier and Dr. Letitia Yao provided assistance with NMR spectroscopic studies. Professors Karsten Meyer (University of Erlangen) and Philippe Buhlmann (University of Minnesota) are thanked for helpful suggestions. We would also like to thank Sigma-Aldrich for a donation of $[Rh(NBD)_2]BF_4$. Funding for this work was provided by the University of Minnesota. Single crystal X-ray diffraction experiments were performed at the X-ray Crystallographic Laboratory in the Chemistry Department of UMN.

■ REFERENCES

(1) Gillie, A.; Stille, J. K. *J. Am. Chem. Soc.* **1980**, *102*, 4933–4941.
(2) Ozawa, F.; Yamamoto, A. *Chem. Lett.* **1981**, *10*, 289–292.
(3) Freixa, Z.; van Leeuwen, P. W. N. M. *Coord. Chem. Rev.* **2008**, *252*, 1755–1786.
(4) Dierkes, P.; van Leeuwen, P. W. N. M. *J. Chem. Soc., Dalton Trans.* **1999**, 1519–1530.
(5) Kamer, P. C. J.; van Leeuwen, P. W. N. M.; Reek, J. N. H. *Acc. Chem. Res.* **2001**, *34*, 895–904.
(6) Birkholz, M.-N.; Freixa, Z.; van Leeuwen, P. W. N. M. *Chem. Soc. Rev.* **2009**, *38*, 1099–1118.
(7) van Leeuwen, P. W. N. M.; Kamer, P. C. J.; Reek, J. N. H.; Dierkes, P. *Chem. Rev.* **2000**, *100*, 2741–2770.
(8) Hamann, B. C.; Hartwig, J. F. *J. Am. Chem. Soc.* **1998**, *120*, 3694–3703.
(9) Bessel, C. A.; Aggarwal, P.; Marschilok, A. C.; Takeuchi, K. J. *Chem. Rev.* **2001**, *101*, 1031–1066.
(10) Smith, D. C., Jr.; Lake, C. H.; Gray, G. M. *Chem. Commun.* **1998**, 2771–2772.
(11) Crocker, C.; Errington, R. J.; Markham, R.; Moulton, C. J.; Odell, K. J.; Shaw, B. L. *J. Am. Chem. Soc.* **1980**, *102*, 4373–4379.
(12) DeStefano, N. J.; Johnson, D. K.; Lane, R. M.; Venanzi, L. M. *Helv. Chim. Acta* **1976**, *59*, 2674–2682.
(13) Freixa, Z.; Beentjes, M. S.; Batema, G. D.; Dieleman, C. B.; van Strijdonck, G. P. F.; Reek, J. N. H.; Kamer, P. C. J.; Fraanje, J.; Goubitz, K.; van Leeuwen, P. W. N. M. *Angew. Chem., Int. Ed.* **2003**, *42*, 1284–1287.
(14) Devon, T. J.; Phillips, G. W.; Puckette, T. A.; Stravinoha, J. L.; Vanderbilt, J. J. . U.S. Patent 4,694,109, Sep 15, 1986.
(15) Kaganovsky, L.; Cho, K.-B.; Gelman, D. *Organometallics* **2008**, *27*, 5139–5145.
(16) Casey, C. P.; Whiteker, G. T.; Melville, M. G.; Petrovich, L. M.; Gavney, J. A.; Powell, D. R. *J. Am. Chem. Soc.* **1992**, *114*, 5535–5543.
(17) van der Veen, L. A.; Keeven, P. H.; Schoemaker, G. C.; Reek, J. N. H.; Kamer, P. C. J.; van Leeuwen, P. W. N. M.; Lutz, M.; Spek, A. L. *Organometallics* **2000**, *19*, 872–883.
(18) Kranenburg, M.; van der Burgt, Y. E. M.; Kamer, P. C. J.; van Leeuwen, P. W. N. M.; Goubitz, K.; Fraanje, J. *Organometallics* **1995**, *14*, 3081–3089.
(19) Brown, A. M.; Ovchinnikov, M. V.; Stern, C. L.; Mirkin, C. A. *J. Am. Chem. Soc.* **2004**, *126*, 14316–14317.
(20) Chisholm, M. H.; Huffman, J. C.; Iyer, S. S. *J. Chem. Soc., Dalton Trans.* **2000**, 1483–1489.
(21) Friebolin, H. *Basic One- and Two-Dimensional NMR Spectroscopy*; VCH: Weinheim, Germany, 1993; pp 47−48.
(22) Allen, F. *Acta Crystallogr., Sect. B* **2002**, *58*, 380–388.
(23) O'Toole, T. R.; Younathan, J. N.; Sullivan, B. P.; Meyer, T. J. *Inorg. Chem.* **1989**, *28*, 3923–3926.
(24) Haefner, S. C.; Dunbar, K. R.; Bender, C. *J. Am. Chem. Soc.* **1991**, *113*, 9540–9553.
(25) Dunbar, K. R.; Haefner, S. C. *Organometallics* **1992**, *11*, 1431–1433.
(26) Casey, C. P.; Whiteker, G. T. *Isr. J. Chem.* **1990**, *30*, 299–304.
(27) Jimenez-Rodriguez, C.; Roca, F. X.; Bo, C.; Benet-Buchholz, J.; Escudero-Adan, E. C.; Freixa, Z.; van Leeuwen, P. W. N. M. *Dalton Trans.* **2006**, 268–278.
(28) Zhao, Y.; Truhlar, D. G. *Acc. Chem. Res.* **2008**, *41*, 157–167.
(29) Schwartz, E. B.; Knobler, C. B.; Cram, D. J. *J. Am. Chem. Soc.* **1992**, *114*, 10775–10784.
(30) Sen, A.; Lai, T. W. *Inorg. Chem.* **1984**, *23*, 3257–3258.
(31) Blessing, R. *Acta Crystallogr., Sect. A: Found. Crystallogr.* **1995**, *51*, 33–38.
(32) *SHELXTL*, V6.10; Bruker Analytical X-Ray Systems: Madison, WI, 2000.
(33) Frisch, M. J.; Trucks, G. W.; Schlegel, H. B.; Scuseria, G. E.; Robb, M. A.; Cheeseman, J. R.; Scalmani, G.; Barone, V.; Mennucci, B.; Petersson, G. A.; Nakatsuji, H.; Caricato, M.; Li, X.; Hratchian, H. P.; Izmaylov, A. F.; Bloino, J.; Zheng, G.; Sonnenberg, J. L.; Hada, M.; Ehara, M.; Toyota, K.; Fukuda, R.; Hasegawa, J.; Ishida, M.; Nakajima, T.; Honda, Y.; Kitao, O.; Nakai, H.; Vreven, T.; J. A. Montgomery, J.; Peralta, J. E.; Ogliaro, F.; Bearpark, M.; Heyd, J. J.; Brothers, E.; Kudin, K. N.; N.Staroverov, V.; Kobayashi, R.; Normand, J.; Raghavachari, K.; Rendell, A.; Burant, J. C.; Iyengar, S. S.; Tomasi, J.; Cossi, M.; Rega, N.; Millam, J. M.; Klene, M.; Knox, J. E.; Cross, J. B.; Bakken, V.; Adamo, C.; Jaramillo, J.; Gomperts, R.; Stratmann, R. E.; Yazyev, O.; Austin, A. J.; Cammi, R.; Pomelli, C.; Ochterski, J. W.; Martin, R. L.; Morokuma, K.; Zakrzewski, V. G.; Voth, G. A.; Salvador, P.; Dannenberg, J. J.; Dapprich, S.; Daniels, A. D.; Farkas, O.; Foresman, J. B.; Ortiz, J. V.; Cioslowski, J.; Fox, D. J. *Gaussian 09*, Revision A.02; Gaussian, Inc.: Wallingford, CT, 2009.
(34) Zhao, Y.; Truhlar, D. G. *J. Chem. Phys.* **2006**, *125*, 194101–194118.
(35) Weigend, F.; Ahlrichs, R. *Phys. Chem. Chem. Phys.* **2005**, *7*, 3297.
(36) Schäfer, A.; Horn, H.; Ahlrichs, R. *J. Chem. Phys.* **1992**, *97*, 2571–2577.